

The analysis of the flying wing in morphing concept

Vasile PRISACARIU*¹, Ionică CÎRCIU²

*Corresponding author

¹“Transilvania” University of Brasov, 1 Colina Universitatii, Braşov
aerosavelli73@yahoo.com

²Air Force Academy “Henri Coandă”, 160 Mihai Viteazu, Braşov
circiu.ionica@yahoo.co.uk

DOI: 10.13111/2066-8201.2013.5.2.6

Abstract: *The combination between the flying wing morphing concept and the use of modern command and control system offers exponential advantages having a leverage effect in the economy and research. The flying wing architecture has the advantage of low cost against efficiency, the morphing of this concept defining the new characteristic frontiers and aerodynamic performances which derive immediately. On designing an unmanned aerial vehicle for a various range of missions, its lifting surface needs to display optimal geometrical features, so that the UAV may maintain the induced drag and the moment coefficient at reasonable levels. The command and control of the lifting surfaces in morphing concept offer characteristics and in-flight performances at a superior level. The limits of the system depend on the reliability of the execution elements and the grade of accuracy for the control laws which are implemented in the calculation module. The paper aims at presenting an analysis regarding the robotic air systems of flying wing type through the aerodynamic analysis and with the help of specific software instruments. The performances and flight qualities depend directly on the geometry of the lifting surface of the aerial vehicle.*

Key Words: *flying wing, stability, morphing, vortex lattice method, Clark YH airfoil*

1. INTRODUCTION

The unmanned aerial vehicle (UAV) had known in the last decades a quick evolution due the miniaturization technology and the market demands. The robotic aerial system is defined as a pilotless aerial vector transporting usable payloads depending on the mission and evolving under the action of the aerodynamic, non-ballistic and manual forces, or by means of an autopilot. Figure 1 shows several types of flying wings belonging to the main categories of UAVs [1].

Over the years unpiloted aerial vectors have achieved a great technological advance which imposed an extension of the searching area together with the growth of the intrinsic and related performances.

An interesting zone delimited by NASA, DARPA and other great university researchers would be the performance study regarding unpiloted airships in the morphing concept. Morphing aircraft offer the advantage of changing the form of the wing during the flight for a better optimization of the performances depending on the mission objectives. Although the benefits of the morphing concept are obvious, from the aerodynamic point of view, the technical realizations are still a critical problem.

The design of a morphing airplane involves new challenges regarding the design method, materials, and command and control elements [2].

The actual use of the classical hyper-sustentation represents a simplification of the morphing concept, these widgets being traditional control systems for limited condition

flight. Outside these conditions the traditional control system is neutral, and can influence negatively the aerodynamic performances or they could have small yield. They are inefficient in the air flux control due to the discontinuous surfaces created by hinges which leads to undesired aerodynamic phenomena [3].













<p>Micro</p>  <p>Aerovironment, USA</p>	<p>Mini</p>  <p>Orbiter, Israel</p>	<p>Close Range</p>  <p>Maxi 10, France</p>	<p>Short Range</p>  <p>Exodrone, USA</p>
<p>Medium Range</p>  <p>Sperwer, France</p>	<p>Medium Range Endurance</p>  <p>Wachkeeper, Israel</p>	<p>Low Altitude Deep Penetration</p>  <p>CL 289, France-Germany</p>	<p>Low Altitude Long Endurance</p>  <p>Eagle Scan, USA</p>
<p>Medium Altitude Long Endurance</p>  <p>Predator A, USA</p>	<p>High Altitude Long Endurance</p>  <p>Global Hawk, USA</p>	<p>Unmanned Combat Aircraft</p>  <p>Cutlass Raytheon, USA-Israel</p>	<p>Optionally piloted, converter UAS</p>  <p>Herti 1D, UK</p>

Figure 1. Main categories of the UAV

The interest area for morphing lifting surfaces has been reduced and they are defined as flight wings with morphing elements (variable airfoil, active winglet, vectorized thrust), see figure 1.

The combination between the flying wing morphing concept and the use of modern command and control system offers exponential advantages having a leverage effect in the economy and research.

The flying wing architecture has the advantage of low cost against efficiency and this concept morphing defines the new characteristic frontiers and aerodynamic performances which derive immediately.

The growth of the flight performances has allowed some evolutions (3D) which were impossible in the past and which now generate unknown aerodynamic phenomena and unknown flight regimes. The regimes can affect the flight security which has generated concerns about how to solve the physical principles and the measures need to be taken to prevent unwanted effects.

According to taxonomy of the morphing concept [4] elaborated till now (Bristol University), we have 2 categories: iso-morphing and poly-morphing which include five categories of morphing according to figure 2.

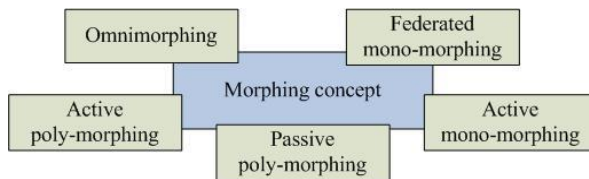


Figure 2. Taxonomy of the morphing concept

2. THEORETICAL REFERENCES

The design of a UAV for a large scale of missions depends on the lifting surface which must present optimal geometry characteristics so it can maintain drag and the coefficient moment at reasonable levels.

Depending on how we obtain longitudinal stability at tailless aircraft we have 3 categories (figure 2) knowing that the requests for the aerodynamic torque coefficient is the direct result of the stability mechanism:

- Plank wing, the longitudinal stability is realized aerodynamically with the help of profile with a positive momentary coefficient $C_m > 0$ (figure 3a);
- Swept wing, the longitudinal stability is realized with a combination between wing torsion and the use of adequate profiles, $C_m \approx 0$ (figure 3b);
- Parafoil wing, the longitudinal stability is realized with a lower position of the gravity center which can use traditional wing forms and profiles, $C_m < 0$ (figure 3c).

The position of the gravity center guarantees longitudinal stability in case it is positioned in front of the neutral point. Thus, amortized dynamic oscillations are obtained.

The research in the flight domain identified a series of phenomena: logical, special and critical [5]. The influence of these phenomena was analyzed through the flight qualities (stability, maneuverability).

The main critical phenomena can appear in the aerial dynamic vectors as a loss of stability during the flight.

We can enumerate a few cases of unstable evolutions which lead to deterioration of the flying envelope and sometimes they can lead to the loss of the aerial vector: loss of the stability direction, the longitudinal balance, self-climbing, moving rotation, landing as a critical flight regime.

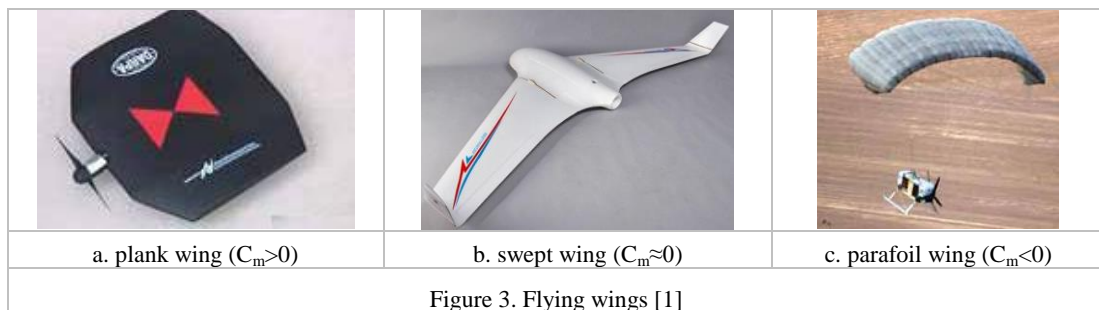


Figure 3. Flying wings [1]

Longitudinal stability/instability of the flying wing

The flight stability implies an analysis of possible movements which can produce and overlap over the specified ground move. If all the disturbed movements remain near the base movement, they will be attenuated and will disappear after all the disruptive factors stop, then we can say the flight is steady [6].

$$M = \frac{\rho}{2} V^2 S \bar{c} \cdot C_m \tag{1}$$

With incidence angle α :

$$M = M(\alpha) \text{ or } C_m = C_m(\alpha) \tag{2}$$

where have: $\frac{\rho}{2} V^2 = \text{const.}$, S – surface, \bar{c} – medium aerodynamic chord.

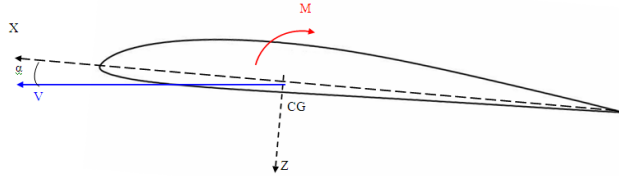


Figure 4. Flying wing – linear and uniform flight

In figure 4 we consider a flying wing with a linear and uniform flight. Here we admit the hypothesis of fixed commands, in other words flaperons are in the correct balanced flight, $M = 0$ ($C_m = 0$), position and blocked in this position. In this case the pitch moment coefficient is a unique angle function. The dependency $C_m = C_m(\alpha)$ is represented in figure 3 the angle being measured from the lift null axe of the flying wing. The sign conventions are: the positive pitch moment increases the incidence and the negative one decreases it, the condition of a flying wing maintaining its incidence α_0 ($C_m = 0$) in linear flight is:

$$\left(\frac{\partial C_m}{\partial \alpha} \right)_{\alpha=\alpha_0} < 0 \tag{3}$$

Developing the function in power series:

$$C_m = C_m(\alpha), \quad C_m = C_{m0} + C_m^\alpha \alpha$$

$$C_m(\alpha) = C_{m0} + \left(\frac{\partial C_m}{\partial \alpha} \right)_0 \alpha + \frac{1}{2!} \left(\frac{\partial^2 C_m}{\partial \alpha^2} \right) \alpha^2 + \dots \tag{4}$$

Having in sight the cvasiliniar dependence, growing, we can retain only the linear terms of the moment coefficient in α :

$$C_m = C_{m0} + \left(\frac{\partial C_m}{\partial \alpha} \right)_0 \alpha \tag{5}$$

So the condition for an airplane to be steady in linear flight is $C_m = 0$, at a positive incidence, $\alpha = \alpha_0$ and to be stable:

$$\begin{aligned} &\left(\frac{\partial C_m}{\partial \alpha} \right)_{\alpha=\alpha_0} < 0 \\ &C_{m0} > 0, \quad C_{m\alpha} = \left(\frac{\partial C_m}{\partial \alpha} \right)_0 < 0 \end{aligned} \tag{6}$$

where C_{m0} - pitching moment coefficient at zero lift ($\alpha=0$), $C_{m\alpha}$ - coefficient of static longitudinal stability

The relations (6) must be satisfied simultaneously so that the airplane could be balanced and stable. For a flying wing to be stable in linear and uniform flight at $\alpha > 0$ it is necessary for $C_{m0} > 0$, which can always be realized when the airplane is equipped with a horizontal tail, but in case of tailless airplane the functions is realized with advanced CG (weight center) compared to the neutral point, choosing an adequate aerodynamic concept (airfoil S) or with a torsion (aerodynamic, geometric) of the tip chord.

Command and control of flying wing type UAV in the morphing concept

The mostly used construction solution for command and longitudinal control of an airplane is the elevator. In the case of longitudinal flying wings command it is realized with the elevons, (see figure 4); this solution is available only for swept wings or triangular wings. In the case of symmetrical airfoils or with positive curb we obtain $C_{m0} > 0$ through the negative geometric torsion in the span. Turning the elevons modifies the pitch and lifting moment, so the dimensionless coefficients of these are the incident angle function α and the turning angle of the elevon δ :

$$C_l = C_l(\alpha, \delta), \quad C_m = C_m(\alpha, \delta) \quad (7)$$

The proposed model is based on the concept of semi-flexibility heads wing offering superior flight performance and the advantage of low cost conditions [7].

3. THE ANALYSIS OF THE FLYING WING TYPE LIFTING SURFACE

We propose to analyze a flying wing surface (figure 5) with the data from table 1 with Clark YH profile composed of 2 semi-plans mounted on a central plan, with a dihedral angle of 0^0 .

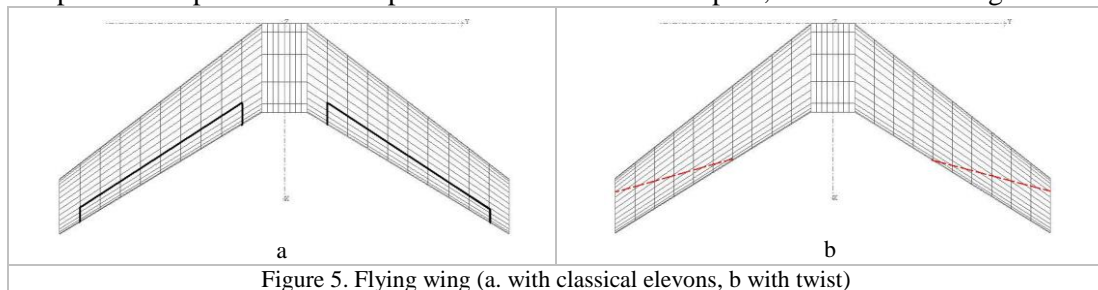


Figure 5. Flying wing (a. with classical elevons, b with twist)

Table 1. Flying wing features:

Wing span	$2b$	2000 mm
Main chord	C_o	400 mm
Tip chord	C_e	250 mm
Medium aerod. chord	MAC	339 mm
Aspect ratio	λ	6,02
Wing weight	G	1,00 kg
Wing load	I	1,504 kg/m ²
Wing area	S	0,665 m ²
Swept angle	χ	35 ⁰

Analysis methodology

XFLR5 v.6 is software that offers an analysis in 2D and 3D for shapes and lifting surfaces in singular and coupled mode [8]. The software package performs analysis for small Reynolds numbers and contains five applications: analysis mode and projection in 2D, analysis method and projection in 3D (wing, airplane), two projection modes and comparison in 2D, inverted projection mode (QDES) and integral projection mode (MDES).

Command through symmetrical geometric twist

According to figure 5, the analyzed wing, displaying the characteristics shown in table 2 has the lifting chart, drag and induced drag through VLM (vortex lattice method) and the analysis which has a specific resolution in the analysis process which is presented in the next figures. The analyzed case represents a symmetrical geometrical twist with 5° .

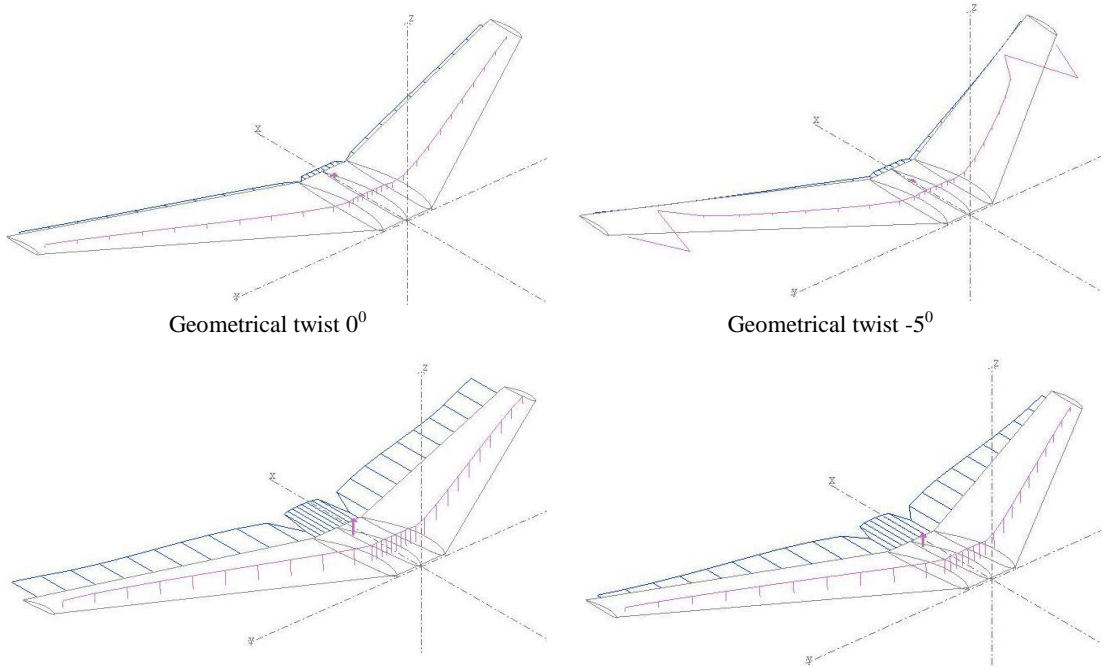


Figure 6. Lifting chart and drag at 15 m/s with 0° și 5° incidence angle.

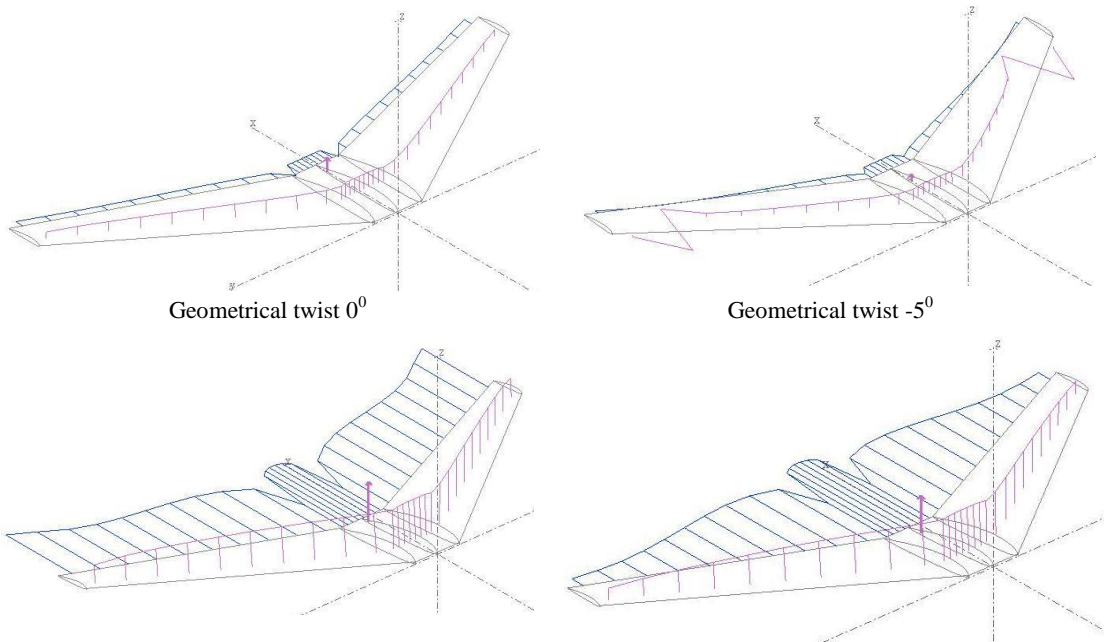


Figure 7. Lifting chart and drag at 25 m/s with 0° and 5° incidence angle

From figure 6 and 7 and according to table 3, as expected, we observe an improvement of the performance of the lifting surface in case of incidence lowering at the wing tip. In table 2 we have values of the lifting coefficients, drag for going forward and for the moment depending on the incidence angle.

Tabelul 2. Coefficients values

Incidence α	Twist 0^0			Twist -5^0		
	C_l	C_d	C_m	C_l	C_d	C_m
-5^0	-0.20401	0.001845	-0.02148	-0.27554	0.004015	0.022706
-2^0	0.020953	0.000026	-0.01882	-0.05802	0.00065	0.017208
0^0	0.171192	0.001306	-0.01694	0.087538	0.000739	0.013549
3^0	0.39544	0.006949	-0.01398	0.305281	0.004382	0.008113
5^0	0.543331	0.13141	-0.01193	0.449218	0.009115	0.004549
7^0	0.689254	0.021205	-0.00982	0.591524	0.0015633	0.001055
10^0	0.90322	0.036612	-0.00658	0.800742	0.028589	-0.00402
15^0	1.242322	0.070088	-0.00106	1.133883	0.057758	-0.0119

4. COMMAND AND CONTROL MODEL THROUGH LONGITUDINAL DRIVELINE

For the stabilization of a flying wing with the reserve of the balance smaller in comparison with the classic design (with tail), we propose a command and control module with a cinematic driveline of the pitch movement for improving the reaction time and the longitudinal trajectory through torsion angle values of $\pm 15^0$. The first element is the airplane, bloc 2 to regroup the control; it is done after ψ , $\dot{\psi}$ and the command δ . The third element performs passive or active correction series and N is the static characteristic of the execution element. In figure 8a and 8b we have the following operators:

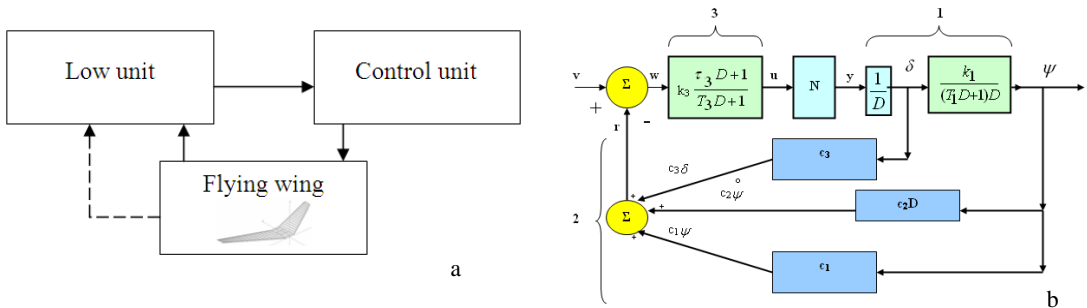


Figure 8 Command and control model

$$H_1(D) = \frac{k_1}{(T_1 + 1)D^2},$$

$$H_2(D) = c_1 + \left(c_2 + \frac{c_3}{k_1} \right) D + \frac{c_3 T_1}{k_1} D^2, \tag{8}$$

$$H_2(D) = k_3 \frac{\tau_3 D + 1}{T_3 D + 1}, \tau_3 \neq T_3.$$

The model proposed (figure 7b) achieves the control after three state variables (incident angles, twist a top wing and aerial speed vector) involving superior dynamic characteristics and performances [9], [10], [11]. To avoid the separated treatment of the differential elements $H_2(D)$ from (8) we will regroup with $H_1(D)$ in an operator $H_{12}(D)$ with the following form:

$$H_{12}(D) = \frac{c_3 T_1 D^2 + (k_1 c_2 + c_3) D + c_1 k_1}{(T_1 D + 1) D^2} \cong \frac{r}{y} \tag{9}$$

We attach to this operator $H_{12}(D)$ a minimal state architecture with accessible variables δ, ψ weighted with the coefficients c_1, c_2, c_3 which are marked even in the minimal architecture. In this architecture the state vector has the following components:

$$\begin{cases} x_1 \cong r = c_1 \psi + c_2 \psi + c_3 \psi \\ x_2 = \overset{\circ}{x}_1 - c_3 T_1 y \\ x_3 = \overset{\circ}{x}_2 + T_1 r - (k_1 c_2 + c_3) y \end{cases}$$

The $H_3(D)$ element from (8) is equivalent with the following relationships:

$$\overset{\circ}{x}^{(3)} = A^{(3)} \overset{\circ}{x}^{(3)} + b^{(3)} w, u = \overset{\circ}{x}^{(3)} + d^{(3)} w, w = v - r$$

In which:

$$\overset{\circ}{x}^{(3)} = u - d^{(3)} w, A^{(3)} = -\frac{1}{T_3}, b^{(3)} = \frac{1}{T_3} (k_3 - 1), c^{(3)} = 1, d^{(3)} = \frac{k_3 \tau_3}{T_3}$$

The state equations of the system:

$$\begin{cases} \overset{\circ}{x} = Ax + by + ep + fv, y = g(u) \\ u = c^T x + dy + h^T p + d^{(3)} v \end{cases}$$

This performs the control after three state variable elements:

$$A = \begin{bmatrix} -\frac{1}{T_1} & 1 & 0 & 0 \\ 0 & 0 & 1 & 0 \\ 0 & 0 & 0 & 0 \\ -\frac{k_3 \tau_3}{T_3^2} (k_3 - 1) & 0 & 0 & \frac{-1}{T_3} \end{bmatrix}, b = \begin{bmatrix} c_3 \\ k_1 c_2 + c_3 \\ T_1 \\ c_1 k_1 \\ T_1 \\ 0 \end{bmatrix}, c = \begin{bmatrix} -\frac{k_3 \tau_3}{T_3} \\ 0 \\ 0 \\ 1 \end{bmatrix}, d = 0,$$

$$f = \begin{bmatrix} 0 \\ 0 \\ 0 \\ \frac{k_3 \tau_3}{T_3} \end{bmatrix}, d^{(3)} = \frac{k_3 \tau_3}{T_3}, p = 0. \tag{10}$$

For linear systems, the correction parallel-oppose through the c_2 and c_3 connections from element 2 is similar to a series correction at level of the element 3:

$$H_{3e} = k_{3e} \frac{b_2 D^2 + b_1 D + b_0}{a_2 D^2 + a_1 D + a_0} \tag{11}$$

which together with operator $H_3(D)$ gives a general correction of the third order for linear systems, such an equivalence being kept rigorously but the dynamic effects remain the same. That is why the connection introduced through the third element can be transferred partially through the reverse connections of the c_2 and c_3 coefficients. Simplifying the third element through:

$$\tau_3 = T_3 = 0 \text{ and } k_3 = I$$

we reduce the closing equation of the system at:

$$\dot{x}_{12} = A_{12}x_{12} + b_{12}y, \quad r = c_{12}^T x_{12}, \quad u = v - r, \quad y = g(u)$$

If the nonlinearity N is replaced with a linear element without a unitary memory path, the equivalent operator $H_{3e}(D)$ has the expression:

$$H_{3e}(D) = \frac{(T_1 D + 1)D}{T_1 D^2 + (1 + c_3 T_1)D + k_1 c_2} \tag{12}$$

In figure 9 we present the command and control module performed in Simulink Matlab 2010 [12], [13].

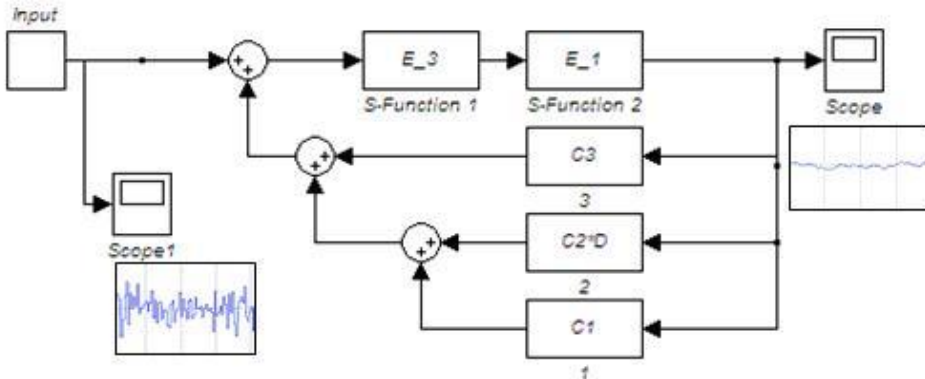


Figure 9. Simulink model

The appearance of the derivative effect does not decouple the direct circuit in stationary regime because this effect is compensated by the first integrator in the first element. In the stability conditions the internal stability is amortized, the nonlinear static characteristic N will affect the counter and partially the denominator of the equivalent operator.

5. CONCLUSIONS

The proposed module represents an upgrade of the control laws and the execution of the existing equipment used on non piloted aerial vectors.

The command and control of the lifting surfaces in the morphing concept offers characteristics and performances at a whole new level. The limits of the control system depend on the reliability of the execution elements and the accuracy level of the implemented control laws in the calculation modules.

The present research is based on the autopilot flight concept without the help of humans in control. The main interest is the correlation between the sensors accuracy, the calculation speed of the hardware platforms and the quick execution of the command elements.

ACKNOWLEDGMENT

The authors wish to thank "Transilvania" University and "Henri Coandă" Air Force Academy of Braşov for supporting the necessary research for writing this article.

REFERENCES

- [1] UAS Yearbook, *Unmanned aircraft systems – The Global Perspective 2011/2012*, Blyenburg & Co, June 2011, Paris, ISSN 1967-1709, 216 p., www.uvs-info.com.
- [2] B. Beguin, C. Breitsamter, N. Adams, Aerodynamic investigation of a morphing membrane wing, *AIAA Journal*, vol **50**, no.11, p2588-2599, nov. 2012.
- [3] S. Barbarino, O. Bilgen, R. M. Ajaj, M. I. Friswell, D. J. Inman, A review morphing aircraft, *Journal of intelligent material system and structures*, vol **22**, p823-877, 2011.
- [4] T. Melin, A. T. Isikveren, M. I. Friswell, *Cost appreciation of morphing uav projects at a conceptual design stage*, p 6., http://michael.friswell.com/PDF_Files/C239.pdf, 2008.
- [5] V. Reghintovschi, *Fenomene și regimuri critice în dinamica și manevrabilitatea aeronavelor militare*, București, 176p, 1991.
- [6] I. Grigore, *Mecanica zborului avionului*, Editura Academiei Militare, 260p, 1987.
- [7] M. Boscoianu, R. Pahonie, A. Coman, *Some Aspects Regarding the Adaptive Control of a Flying Wing-Micro Air Vehicle with Flexible Wing Tips*, Conference on MATHEMATICAL METHODS AND COMPUTATIONAL TECHNIQUES IN ELECTRICAL ENGINEERING (MMACTEE'08), Sofia, Bulgaria, 6p, May 2-4, 2008.
- [8] *Guidelines for XFLR5 v6.03*, 2011, 71p., www.xflr5.com consulted at 16.12.2012.
- [9] M. Voicu, *Introducere în automată*, Editura Polirom, ISBN 973-681-111-5, 280 p, 2002.
- [10] M. Lungu, L. Lungu, C. Rotaru, New Systems for Identification, Estimation and Adaptive Control of the Aircrafts Movement, *Studies in Informatics and Control*, vol **20**, no.3, 12p, www.sic.ici.ro, 2011.
- [11] Ioan URSU, The kinematics of the rigid feedback linkage, the impedance of the hydraulic servomechanism and the flutter occurrence, *INCAS BULLETIN*, Volume **4**, Issue 3, (online) ISSN 2247-4528 (print) ISSN 2066-8201, ISSN-L 2066-8201, <http://bulletin.incas.ro>, pp. 63 – 69, 2012.
- [12] *Simulink basics tutorial*, 26 p. http://faculty.uml.edu/pavitabile/22.457/UMICH_Simulink_Tutorial.pdf, consulted at 01.02.2013.
- [13] <http://pundit.pratt.duke.edu/wiki/Simulink/Tutorials/Signals>, consulted at 01.02.2013.